

Multiconfigurational Self-Consistent Field Calculations of the Magnetically Induced Current Density Using Gauge-Including Atomic Orbitals

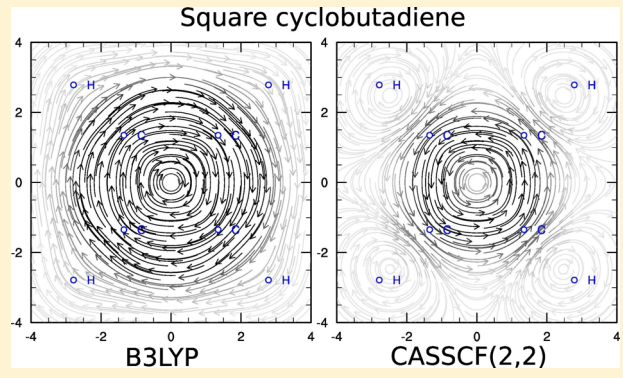
Shubhrodeep Pathak,[†] Radovan Bast,[‡] and Kenneth Ruud^{*,§}

[†]Raman Center for Atomic, Molecular and Optical Sciences, Indian Association for the Cultivation of Science, Kolkata 700 032, India

[‡]Laboratoire de Chimie et Physique Quantiques (UMR 5626), CNRS/Université de Toulouse 3 (Paul Sabatier), 118 route de Narbonne, F-31062 Toulouse, France

[§]Centre for Theoretical and Computational Chemistry, Department of Chemistry, University of Tromsø, N–9037 Tromsø, Norway

ABSTRACT: Nondynamical electron correlation based on a genuine multiconfigurational theory is of considerable importance for a balanced *ab initio* calculation of aromatic and antiaromatic molecules either with open-shell character or quasi-degeneracy in the electronic states. Among the various aromaticity indices, the calculation of magnetically induced ring current densities (MICD) has emerged as a strong contender, providing both a qualitative and a quantitative description of the effect. We report here the first implementation of MICD at the multiconfigurational self-consistent field (MCSCF) level of theory together with example calculations. This extension makes the method applicable to systems that cannot be appropriately handled with earlier implementations based on a single-reference starting function. We present the formulation of the MCSCF MICD theory along with applications to a prototypical antiaromatic (cyclobutadiene) and an aromatic (benzyne) system, both systems that require a multiconfigurational description. We compare the MCSCF results to those obtained using Hartree–Fock and Kohn–Sham density functional theory and discuss the effects of static correlation on the aromaticity.



1. INTRODUCTION

Aromaticity has been a central concept in chemistry^{1–3} since the first isolation of benzene, and although several attempts have been made to describe this concept qualitatively and quantitatively, aromaticity still eludes a clear definition and remains a fascinating area of much activity and debate. There are four main classes of aromaticity indices, focusing on structural parameters,^{2,4,5} energetics,^{6–8} reactivity,^{9,10} and magnetic properties,^{11–18} respectively.

Starting with the ring-current theory of Pauling¹² and the subsequent advances, the magnetic criterion^{19,20} is today the most widely explored method and probably the most generally transferable aromaticity index due to its straightforward quantification without the need for reference values from hypothetical structures. The magnetic criterion used to rely on characteristic diamagnetic susceptibility exaltations^{11,14,21} and unique chemical shifts,^{22–24} conforming with the fact that aromaticity has been defined as an “excess property”. The unusually high values of magnetic susceptibility anisotropies and exaltations in the case of susceptibility measurements as well as the characteristic diatropic shifts for exocyclic protons and paratropic shifts for the endocyclic protons in the case of NMR studies can be attributed to a net diamagnetic ring current^{13,25} of the delocalized electrons in the molecular

framework when an external magnetic field is applied. Bilde and Hansen have pointed out that this diamagnetic ring current is due to the quenching of the paratropic current, indicating that this criterion measures the flow of π electrons in a near-circular geometric shape for which the magnetic moment around the perpendicular axis vanishes.²⁶ The magnetic criterion has led to a search for a method for the direct quantitative determination of the ring current strength,^{18,23,24,27} giving a more applicable measure of electron delocalization and hence of the aromatic character than the two other magnetic criteria mentioned above.

Lazzeretti and Zanasi^{17,28} introduced the concept of *ab initio* current density plots, which opened a new direction in terms of a qualitative estimation of the electron flow in a ring structure. Using *ab initio* current density plots, Jusélius et al.²⁹ have presented a method for quantifying aromaticity by integrating the induced current susceptibility passing through specific planes. This approach has become a reliable aromaticity index allowing for a quantitative determination and comparison of the extent of electron delocalization. The gauge-including magnetically induced currents (GIMIC) method has since been applied

Received: December 21, 2012

to determine the aromacity or antiaromaticity of many different ring systems at various levels of theory,^{29,30} such as Hartree–Fock (HF) and Kohn–Sham (KS) self-consistent field levels as well as higher-order correlated methods such as coupled-cluster singles-and-doubles with perturbative or full triples, CCSD(T) or CCSDT, respectively. Bast et al. presented a four-component relativistic implementation of the magnetically induced current density (MICD) using a common gauge origin³¹ approach. Later, this implementation was extended by Sulzer et al. to use gauge-including atomic orbitals.³²

All previous MICD calculations were performed using single-reference methods. This means that although the effects of dynamic correlation on the MICD have been studied, static electron correlation effects have not been considered because an implementation for multiconfigurational wave functions was not available. The inclusion of static correlation becomes important in systems with open-shell ground and excited states, near-degenerate closed-shell ground states, multiple bonds, stretched bonds, and those involving atoms with partially filled electronic levels. These bonding situations are characterized by a strong interplay between various electronic configurations close in energy, bringing in a considerable amount of static electron correlation and requiring the use of a multiconfigurational self-consistent field (MCSCF) wave function.³³

In this paper we present the implementation and example applications of the MICD at the MCSCF level of theory in order to extend the applicability of this promising method to a host of systems hitherto unapproachable due to the multiconfigurational nature of the states considered. Our implementation is based on the multiconfigurational linear response (MCLR) theory, which from its first formulation by Yeager and Jørgensen³⁴ and later improvements,^{35,36} has been extensively applied to a variety of electric and magnetic properties, such as vibrational circular dichroism,³⁷ nuclear magnetic shielding constants,³⁸ and magnetizabilities³⁹ to mention only a few.

The MCSCF linear response equations are gauge invariant in the limit of a complete basis set.³⁵ In the case of a truncated basis set, which we are bound to use in standard quantum-chemical computations, the results are no longer gauge invariant, and they are in particular not gauge-origin independent. For computations on symmetric cyclic systems or similar structures, a common gauge origin can be chosen for the sake of comparison of relative aromacities. However, when we aim to establish a transferable index of aromaticity or degree of electron delocalization, we strive for results which are independent of the choice of gauge origin. We have therefore implemented our method using gauge-including atomic orbitals (GIAO), also known as London atomic orbitals (LAO),^{26,38,40–42} which provide a convenient way to bypass the problem of gauge-origin dependence and hence gives us the opportunity to compare the values of integrated current densities obtained in different chemical systems. An added benefit of using GIAOs is the much improved basis set convergence, which becomes particularly important for computationally expensive methods such as the MCSCF approach.⁴³

In the next section, we outline the derivation of the current density expressions and the theory of MICD using the unperturbed and modified density matrices from the MCLR equations. In Section 3 we present the computational details. In Section 4 we present applications to one antiaromatic molecule (cyclobutadiene) and a set of aromatic molecules (*ortho*-, *meta*-, and *para*-benzenes), all systems displaying considerable multi-

reference character. We summarize and present concluding remarks in Section 5.

2. THEORY

We will present the methodology in two steps. In the first subsection we will derive a general expression for the magnetically induced current density in the atomic-orbital (AO) basis, without providing all technical details of the so-called relaxation contribution, keeping it generic with respect to the choice of an SCF or MCSCF reference state. The relaxation term will be detailed in the second subsection, where we discuss the construction of the first-order perturbed one-electron density matrix, which is the key ingredient for obtaining the working equations for the paramagnetic contribution to the MICD at the MCSCF level of theory.

2.1. Magnetically Induced Current Density. In deriving the expression for the magnetically induced current density, it is convenient to start from the nonrelativistic, one-electron Hamiltonian in the presence of the external vector and scalar potentials, \vec{A} and V , respectively

$$h = \frac{(\vec{p} + \vec{A})^2}{2} - V \quad (1)$$

In this equation and throughout this paper we will use atomic units, thus omitting the explicit electron mass $m_e = 1$ and electron charge $e = 1$. Before introducing the external magnetic field, we can expand eq 1 to obtain four contributions

$$h = \frac{1}{2}\vec{p}^2 + \frac{1}{2}(\vec{p} \cdot \vec{A} + \vec{A} \cdot \vec{p}) + \frac{1}{2}\vec{A}^2 - V \quad (2)$$

two of which depend on the vector potential \vec{A} . In the following, we will limit ourselves to consider only the interaction part of the Hamiltonian where we retain only the terms which depend on \vec{A} and V

$$h_{\text{int}} = \frac{1}{2}(\vec{p} \cdot \vec{A} + \vec{A} \cdot \vec{p}) + \frac{1}{2}\vec{A}^2 - V \quad (3)$$

The expectation value of this Hamiltonian is the interaction energy functional

$$E_{\text{int}} = \langle \psi | h_{\text{int}} | \psi \rangle = \int d\vec{r} [n(\vec{r})V(\vec{r}) - \vec{j}(\vec{r}) \cdot \vec{A}(\vec{r})] \quad (4)$$

from which we can identify the expression for the current density $\vec{j}(\vec{r})$ by taking a functional derivative of the interaction energy E_{int} with respect to \vec{A}

$$\begin{aligned} \vec{j}(\vec{r}') = & - \int d\vec{r} \left[\frac{1}{2} \psi^* \vec{p} \delta(\vec{r} - \vec{r}') \psi + \frac{1}{2} \psi^* \delta(\vec{r} - \vec{r}') \vec{p} \psi \right. \\ & \left. + \vec{A} \psi^* \delta(\vec{r} - \vec{r}') \psi \right] \end{aligned} \quad (5)$$

We will use $\vec{p} = -i\vec{\nabla}$ and by integrating by parts move the differentiation from $\delta(\vec{r} - \vec{r}')$ in the first right-hand side term of eq 5 to the wave function, and obtain

$$\begin{aligned} \vec{j}(\vec{r}) = & \frac{i}{2} [-(\vec{\nabla} \psi^*(\vec{r})) \psi(\vec{r}) + \psi^*(\vec{r}) (\vec{\nabla} \psi(\vec{r}))] \\ & - \vec{A} \psi^*(\vec{r}) \psi(\vec{r}) \end{aligned} \quad (6)$$

In the following we will drop the explicit position dependence for notational clarity and swap the first and second right-hand side terms

$$\vec{j} = \frac{i}{2} [\psi^*(\vec{\nabla}\psi) - (\vec{\nabla}\psi^*)\psi] - \vec{A}\psi^*\psi \quad (7)$$

We can now take the step to the molecular orbital (MO) picture in which we will be able to accommodate both SCF and MCSCF theories by using the MO density matrix which has a general definition irrespective of the choice of method

$$D_{pq}^0 = \langle \psi | E_{pq} | \psi \rangle \quad (8)$$

using

$$E_{pq} = a_p^\dagger a_q \quad (9)$$

where p and q are general molecular orbital labels. The current density expression eq 7 can now be written in the MO basis as

$$\vec{j} = \frac{i}{2} \sum_{pq} D_{pq}^0 [\phi_p^*(\vec{\nabla}\phi_q) - (\vec{\nabla}\phi_p^*)\phi_q] - \vec{A} \sum_{pq} D_{pq}^0 \phi_p^* \phi_q \quad (10)$$

For closed-shell systems, the unperturbed current density is zero everywhere. In this article, we are however interested in the first-order derivative of the current density with respect to the external magnetic field (evaluated at zero field strength). For this we will introduce a uniform static magnetic dipole field \vec{B} through a purely transversal vector potential given by

$$\vec{A}_G(\vec{r}) = \frac{1}{2} \vec{B} \times (\vec{r} - \vec{G}) \quad (11)$$

where \vec{G} denotes the position of the so-called gauge origin. To obtain the first-order perturbed magnetically induced current density, we differentiate the expression for the current density with respect to the static magnetic field \vec{B}

$$\vec{j}^{\vec{B}} = \frac{d}{d\vec{B}} \vec{j} \Big|_{\vec{B}=0} = \vec{j}_{\text{para}}^{\vec{B}} + \vec{j}_{\text{dia}}^{\vec{B}} \quad (12)$$

where the paramagnetic part

$$\vec{j}_{\text{para}}^{\vec{B}} = \frac{i}{2} \sum_{pq} D_{pq}^0 [\phi_p^*(\vec{\nabla}\phi_q) - (\vec{\nabla}\phi_p^*)\phi_q] \quad (13)$$

requires the first-order magnetically perturbed density matrix, whereas the diamagnetic part

$$\vec{j}_{\text{dia}}^{\vec{B}} = -\frac{d\vec{A}}{d\vec{B}} \Big|_{\vec{B}=0} \sum_{pq} D_{pq}^0 \phi_p^* \phi_q \quad (14)$$

is evaluated using the unperturbed density matrix D_{pq}^0 .

Now we turn our attention to the problem of the gauge origin dependence of the MICD values. In order to obtain an expression for the MICD which is independent of the position of the gauge origin, we expand the molecular orbitals in a set of LAOs

$$\phi_p = \sum_{\mu} \omega_{\mu} c_{\mu p} \quad (15)$$

where the LAOs are defined as⁴⁰

$$\omega_{\mu}(\vec{r}) = \exp[i\vec{A}_G(\vec{R}_{\mu}) \cdot \vec{r}] \chi_{\mu}(\vec{r}) \quad (16)$$

With this definition both the AOs and the MOs become explicitly field dependent. The field-dependence of the MOs requires the evaluation of a so-called reorthonormalization contribution using an orbital connection to ensure that the MOs remain orthonormal at all field strengths.⁴⁴ We can write

these orthonormalized MOs (OMOs) $\tilde{\phi}_p(\vec{B})$ as a linear transformation acting on the MOs optimized in the absence of the magnetic field (but which are still magnetic-field dependent through the LAOs)

$$\tilde{\phi}_p(\vec{B}) = \sum_q \phi_q U_{qp}(\vec{B}) \quad (17)$$

As a consequence of the field dependence of the AOs and the use of OMOs, the paramagnetic contribution becomes a sum of two terms

$$\begin{aligned} j_{\alpha;\text{para}}^{B_{\beta}} &= -\frac{1}{4} \sum_{\mu\nu} D_{\nu\mu}^0 [\vec{r} \times (\vec{R}_{\mu} - \vec{R}_{\nu})]_{\beta} [(\nabla_{\alpha}\chi_{\mu}^*)\chi_{\nu} \\ &\quad - \chi_{\mu}^*(\nabla_{\alpha}\chi_{\nu})] + \frac{i}{2} \sum_{\mu\nu} [D_{\nu\mu}^{B_{\beta}} \\ &\quad + T_{\nu\mu}^{B_{\beta}}] [(\nabla_{\alpha}\chi_{\mu}^*)\chi_{\nu} - \chi_{\mu}^*(\nabla_{\alpha}\chi_{\nu})] \end{aligned} \quad (18)$$

The first term involves the direct differentiation of the AOs, whereas the second contains the orbital relaxation contribution and the reorthonormalization term. The latter is given by

$$T_{\nu\mu}^{\vec{B}} = \sum_{pq} c_{\nu p} [\lambda_p \sum_{\kappa} c_{\kappa p}^* \langle \omega_{\kappa}^{\vec{B}} | \phi_q \rangle + \lambda_q \sum_{\kappa} \langle \phi_p | \omega_{\kappa}^{\vec{B}} \rangle c_{\kappa q}] c_{\mu q}^* \quad (19)$$

The paramagnetic contribution requires the evaluation of the unperturbed and the first-order magnetically perturbed AO density matrix elements given by

$$D_{\nu\mu}^0 = \sum_{pq} c_{\nu p} \lambda_p \delta_{pq} c_{\mu q}^* = \sum_p c_{\nu p} \lambda_p c_{\mu p}^* \quad (20)$$

$$D_{\nu\mu}^{B_{\beta}} = \sum_{pq} c_{\nu p} W_{pq}^{B_{\beta}} c_{\mu q}^* \quad (21)$$

where λ_p are the fractional orbital occupation numbers ($0 \leq \lambda_p \leq 2$). The diamagnetic contribution only involves the unperturbed AO density matrix

$$j_{\alpha;\text{dia}}^{B_{\beta}} = -\frac{1}{2} \epsilon_{\alpha\beta\gamma} \sum_{\mu\nu} D_{\nu\mu}^0 (r_{\gamma} - R_{\nu;\gamma}) \chi_{\mu}^* \chi_{\nu} \quad (22)$$

We would like to point out that up to this stage the working formulas for the MICD are applicable to both SCF and MCSCF models. In the following section we shall detail and discuss the construction of the so far unspecified perturbed MO density matrix $W_{pq}^{\vec{B}}$ in the case of an MCSCF wave function.

2.2. Construction of the Perturbed Density Matrix at the Multiconfigurational Self-Consistent Field Level. The construction of the perturbed one-electron density matrix at the MCSCF level of theory is the key ingredient for the computation of the MCSCF MICD. The main difference from the single-reference-based theory is that there are two electronic parameters, one for orbital rotations and one for configuration rotations. Both of these will contribute to the response of the wave function when an external field is applied. To start with, we can write the optimized multiconfigurational wave function at zero field strength as

$$|0\rangle = \sum_g C_{g0} |\Phi_g\rangle \quad (23)$$

where C_{g0} are the expansion coefficients for the set of configuration state functions $|\Phi_g\rangle$, created as linear combina-

tions of Slater determinants. The perturbed MCSCF wave function can be represented in an exponentially parametrized form as^{44,45}

$$|\tilde{0}(\vec{B})\rangle = \exp[-ik(\vec{B})] \exp[-iS(\vec{B})] |0\rangle \quad (24)$$

where the two factors represent the orbital and configurational response, respectively, carried by the orbital rotation and configurational rotation operators

$$\kappa(\vec{B}) = \kappa_{rt}(\vec{B})E_{rt} + \kappa_{rt}^*(\vec{B})E_{tr} \quad (25)$$

$$S(\vec{B}) = S_n(\vec{B})R_n^\dagger + S_n^*(\vec{B})R_n \quad (26)$$

The configurational state transfer parameters are defined as

$$R_n = |0\rangle\langle nl \quad n > 0 \quad (27)$$

$$R_n^\dagger = |nl\rangle\langle 0| \quad (28)$$

where $\{|n\rangle\}$ forms the orthogonal component to the reference CSF $|0\rangle$, and n used as a summation index later in the text denotes summation over all such CSF's in the orthogonal space.

We are interested in the first-order derivative of the MCSCF wave function with respect to the external magnetic field (at zero field strength) in terms of derivatives of the field-dependent operators $\kappa(\vec{B})$ and $S(\vec{B})$,

$$\frac{d}{d\vec{B}} |\tilde{0}(\vec{B})\rangle = [-i \sum_{rt} \kappa_{rt}^{\vec{B}} E_{rt} - i \sum_n S_n^{\vec{B}} R_n^\dagger] |0\rangle \quad (29)$$

A combined response vector $N^{\vec{B}}$ can be introduced, consisting of the response vectors from both the orbital and configurational rotation parts. Following the MCLR formulation in refs 35 and 36, the combined response vector $N^{\vec{B}}$ can be written in a supercolumn vector

$$N^{\vec{B}} = \begin{bmatrix} S_n^{\vec{B}} \\ \kappa_{rt}^{\vec{B}} \\ S_n^{*\vec{B}} \\ \kappa_{rt}^{*\vec{B}} \end{bmatrix} \quad (30)$$

where the orbital rotation parameters κ_{rt} span only the nonredundant sectors. It can be shown that the only nonredundant orbital rotation amplitudes are κ_{ia} (occupied-active), κ_{is} (occupied-secondary), and κ_{as} (active-secondary).⁴⁶ To obtain the response vector via the MCLR scheme, we solve the following equation by iterative techniques³⁶

$$E^{[2]} N^{\vec{B}} = E^{[1]} \quad (31)$$

where $E^{[1]}$ is the property gradient, and $E^{[2]}$ is the electronic Hessian. We refer the reader to the papers by Olsen and Jørgensen³⁵ and by Jørgensen, Jensen, and Olsen³⁶ for the details of MCLR theory as well as Ruud et al. in the specific case of magnetic perturbations.^{38,39} For the discussion of our implementation, we assume that the components $B_n^{\vec{B}}$ and $\kappa_{rt}^{\vec{B}}$ are available (on disk). We will now use these parameters to construct the elements of the first-order perturbed MO density matrix $W_{pq}^{\vec{B}}$ which will have two contributions corresponding to the two contributions of eq 29, the orbital part and the configurational part, recalling that there is also a contribution arising from the orbital connection part in eq 19. For the sake

of notational convenience, we extract the imaginary i from the two contributions in eq 29 and write

$$W_{pq}^{\vec{B}} = iW_{pq}^{\vec{B};\text{orb}} + iW_{pq}^{\vec{B};\text{conf}} \quad (32)$$

We detail the expressions for the contributions $W_{pq}^{\vec{B};\text{orb}}$ and $W_{pq}^{\vec{B};\text{conf}}$ in the next subsections.

2.2.1. Orbital Contribution $W_{pq}^{\vec{B};\text{orb}}$. Before deriving the orbital response contribution $W_{pq}^{\vec{B};\text{orb}}$ in the AO basis, we note that we can excite both into the active orbital space as well as out of this orbital space. This is taken care of by only using nonredundant excitations and using fractional occupation numbers. We write $W_{pq}^{\vec{B};\text{orb}}$ as

$$\begin{aligned} W_{pq}^{\vec{B};\text{orb}} &= \langle 0| \sum_{rt} \kappa_{rt}^{*\vec{B}} E_{tr} E_{pq} |0\rangle - \langle 0| E_{pq} \sum_{rt} \kappa_{rt}^{\vec{B}} E_{rt} |0\rangle \\ &= \sum_{rt} [\langle 0| E_{tr} E_{pq} |0\rangle \kappa_{rt}^{*\vec{B}} - \langle 0| E_{pq} E_{rt} |0\rangle \kappa_{rt}^{\vec{B}}] \end{aligned} \quad (33)$$

Using anticommutation rules for second quantization operators, we can write the excitation operators of eq 33 as

$$E_{tr} E_{pq} = a_t^\dagger a_q \delta_{rp} - a_t^\dagger a_p^\dagger a_r a_q \quad (34)$$

$$E_{pq} E_{rt} = a_p^\dagger a_t \delta_{qr} - a_p^\dagger a_r^\dagger a_q a_t \quad (35)$$

Considering that the index t spans inactive and active orbitals and that the index r spans active and secondary orbitals, we see that only one-body terms contribute to the expectation value. Hence, eq 33 can be written

$$\begin{aligned} W_{pq}^{\vec{B};\text{orb}} &= \sum_{rt} [\langle 0| a_t^\dagger a_q |0\rangle \delta_{rp} \kappa_{rt}^{*\vec{B}} - \langle 0| a_p^\dagger a_t |0\rangle \delta_{qr} \kappa_{rt}^{\vec{B}}] \\ &= \sum_{rt} [\lambda_q \delta_{tq} \delta_{rp} \kappa_{rt}^{*\vec{B}} - \lambda_p \delta_{pt} \delta_{qr} \kappa_{rt}^{\vec{B}}] \\ &= \lambda_q \kappa_{pq}^{*\vec{B}} - \lambda_p \kappa_{qp}^{\vec{B}} \end{aligned} \quad (36)$$

Finally, since the orbital rotation vector is symmetric for static magnetic perturbations, we can use $\kappa_{pq}^{*\vec{B}} = \kappa_{qp}^{\vec{B}}$. With this we can write the final expression for $W_{pq}^{\vec{B};\text{orb}}$ as

$$W_{pq}^{\vec{B};\text{orb}} = (\lambda_q - \lambda_p) \kappa_{qp}^{\vec{B}} \quad (37)$$

This means that $W_{pq}^{\vec{B};\text{orb}}$ has the structure

$$W_{ia}^{\vec{B};\text{orb}} = -\lambda_i \kappa_{ia}^{\vec{B}} + \lambda_a \kappa_{ia}^{\vec{B}} = -W_{ai}^{\vec{B};\text{orb}} \quad (38)$$

$$W_{is}^{\vec{B};\text{orb}} = -\lambda_i \kappa_{is}^{\vec{B}} = -W_{si}^{\vec{B};\text{orb}} \quad (39)$$

$$W_{as}^{\vec{B};\text{orb}} = -\lambda_a \kappa_{as}^{\vec{B}} = -W_{sa}^{\vec{B};\text{orb}} \quad (40)$$

$$W_{ij}^{\vec{B};\text{orb}} = W_{ab}^{\vec{B};\text{orb}} = W_{st}^{\vec{B};\text{orb}} = 0 \quad (41)$$

We can compare this general formula with the SCF level relaxation matrix where the only nonzero blocks are those between inactive and secondary orbitals. No active orbitals are involved in the SCF case

$$W_{is}^{\vec{B};\text{SCF}} = -2\kappa_{is}^{\vec{B};\text{SCF}} = -W_{si}^{\vec{B};\text{SCF}} \quad (42)$$

$$W_{ij}^{\vec{B};\text{SCF}} = W_{st}^{\vec{B};\text{SCF}} = 0 \quad (43)$$

2.2.2. Configurational Contribution $W_{pq}^{\vec{B};\text{conf}}$. A complete active space SCF (CASSCF) wave function performs a full

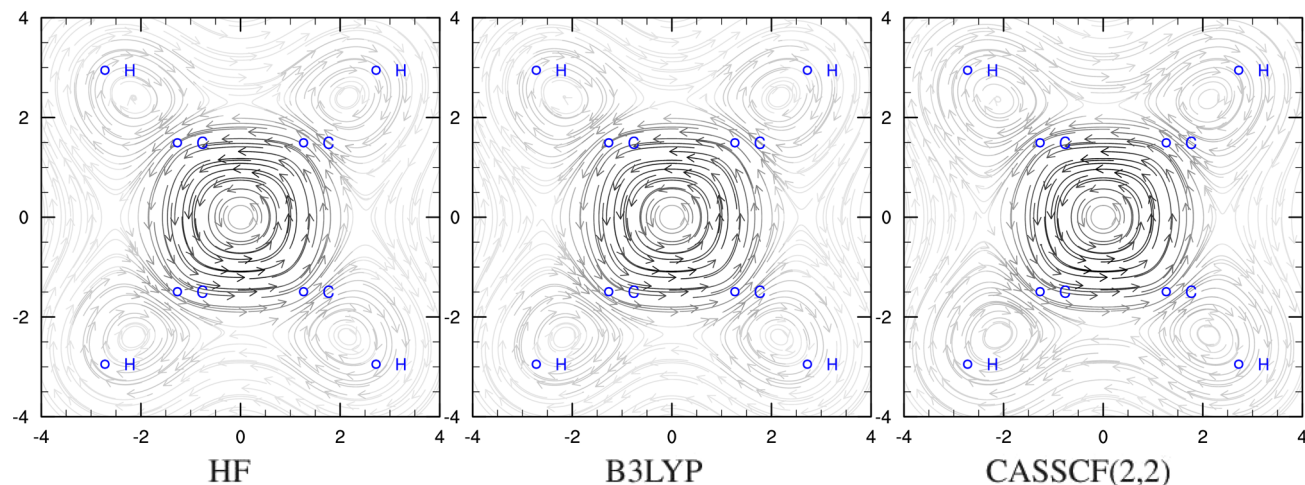


Figure 1. Comparison of MICD plots for rectangular cyclobutadiene plotted $1 \text{ } a_0$ above the molecular plane. The dimensions of the plot are $8 \times 8 \text{ } a_0$. The magnetic field dipole vector is directed toward the reader. The vector arrow color intensity is proportional to the norm of the current density vector.

configuration-interaction optimization within the active space. For this reason, the total configuration part, the active–active block of the perturbed density matrix can be calculated using the configurational rotation parameters alone

$$\begin{aligned} W_{pq}^{\text{conf}} &= \langle 0 | \sum_n S_n^{*\vec{B}} R_n E_{pq} | 0 \rangle - \langle 0 | E_{pq} \sum_n S_n^{\vec{B}} R_n^\dagger | 0 \rangle \\ &= \langle 0^L | E_{pq} | 0^R \rangle + \langle 0^R | E_{pq} | 0^L \rangle \end{aligned} \quad (44)$$

where we have used the notation

$$\langle 0^L | = \langle 0 | \sum_n S_n^{*\vec{B}} R_n = \sum_n S_n^{*\vec{B}} \langle n | \quad (45)$$

$$| 0^R \rangle = - \sum_n S_n^{\vec{B}} R_n^\dagger | 0 \rangle = - \sum_n S_n^{\vec{B}} | n \rangle \quad (46)$$

3. COMPUTATIONAL DETAILS

We have implemented the calculation of MICD at the MCSCF level of theory presented in the previous section in a development version based on the 2011 version of the Dalton program package.⁴⁷ To assess the applicability of our implementation, we have computed the MICD for one classic antiaromatic and a family of aromatic systems with pronounced multireference character, namely cyclobutadiene and the didehydrobenzene (benzyne) family. The structures were optimized at the CASSCF level of theory with the aug-cc-pVDZ basis set using Dalton 2011.⁴⁷ An active space of 2 electrons in 2 active orbitals was used in case of cyclobutadiene. The benzyne isomers were optimized with a much larger active space consisting of 8 electrons in 8 orbitals.

The induced current densities were computed using HF, KS DFT (using the B3LYP functional⁴⁸), and using CASSCF wave functions, all calculations using Dunning's aug-cc-pVDZ basis sets^{49,50} which have been shown to give excellent results for magnetizabilities using GIAOs.^{51,52} To obtain the current densities, we have first performed response calculations at the CASSCF level using GIAOs, with the perturbation operator being a magnetic dipole operator placed perpendicular to the plane in which the current density is computed. The response vector is then read from the file and used to construct the

necessary AO density matrices for the calculation of the induced current densities by the procedure detailed in the previous section.

Induced ring-current susceptibilities were integrated using a 2-dimensional Gauss–Lobatto quadrature grid as discussed in ref 29. The plane of integration was chosen perpendicular to the molecular plane, extending 10 bohr above, below and outward of the ring center. The ring center was defined as the center of mass for all the molecules except *meta*-benzyne, where it was defined as the center of mass considering only the carbon atoms. This integration plane was subdivided in 20 tiles, and each tile was integrated to polynomial order 6. The streamline plots were obtained using the program PyNGL.⁶⁵

4. RESULTS AND DISCUSSION

In the following we will present an analysis of aromaticity using current density streamline plots as well as numerically integrated ring-current susceptibilities using varying active spaces in order to assess the importance of a multiconfigurational description and the dependence of the results on the choice of active space for these systems.

4.1. Cyclobutadiene. Cyclobutadiene can be considered a paradigmatic system for antiaromaticity.⁵³ This system has regularly been the subject of both experimental as well as theoretical studies during the last 40 years.⁵⁴ The antiaromaticity can be deduced from Hückel's $4n-\pi$ electron rule and was indeed later verified by several computational studies using different aromaticity criteria.^{55,56} The reason for the immense difficulty in obtaining cyclobutadiene and getting decent measurements is often attributed to antiaromatic destabilization.⁵⁷ In a recent paper, Wu et al. argue that the destabilization originates from angle strain, torsional strain, and also $\pi-\pi$ and $\sigma-\sigma$ repulsions but there is no doubt about the "magnetic" antiaromaticity.⁵⁸ There is also much controversy about the issue of automerization. Two equivalent rectangular structures of D_{2h} symmetry are said to flip from one state to the other through a square D_{4h} structure. Measurements by Carpenter⁵⁹ suggested barrier heights between 6.7 and 40 kJ/mol. Low-temperature NMR measurements revealed a very high rate of interconversion and placed the activation barrier at about 4 kJ/mol.⁶⁰ Carpenter⁶¹ proposed the possibility of heavy-element tunneling being the preferred pathway below temperatures of 0

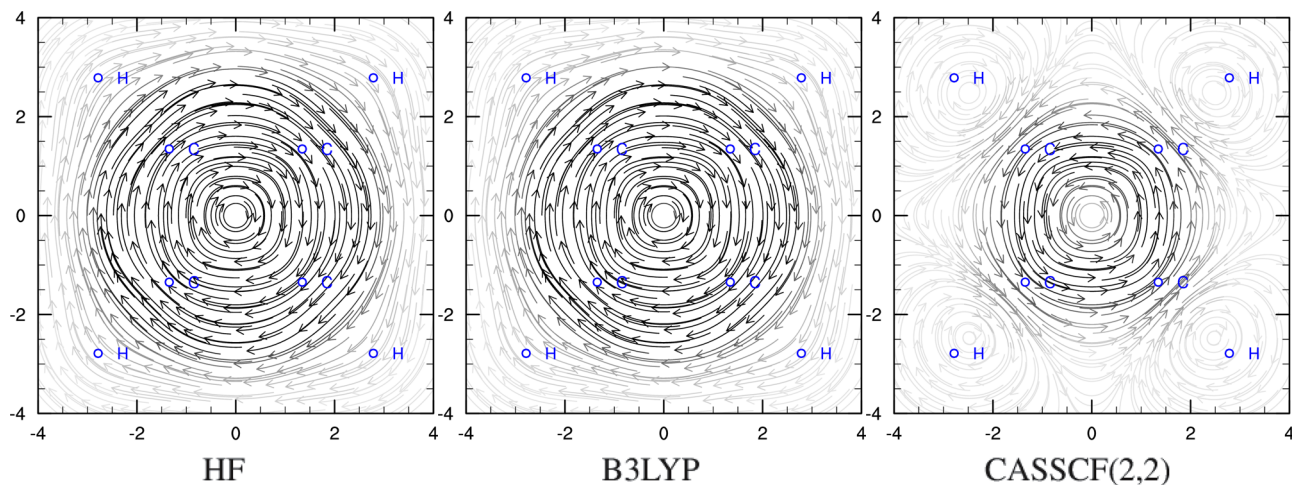


Figure 2. Comparison of MICD plots for square cyclobutadiene plotted $1 \text{ } a_0$ above the molecular plane. Same plot parameters are used as in Figure 1.

^oC. This proposal, although facing some criticism,⁶² has not been abandoned.^{63,64}

Cyclobutadiene has been a challenging system for theoretical chemists as well and very recent high-level computations with multireference theories^{66–68} on this molecule are indicative of the continued interest in understanding the electronic structure of this molecule. The transition from the rectangular to the square structure brings the HOMO π and LUMO π^* very close to each other, both being exactly degenerate at the D_{4h} structure. This makes the square structure impossible to treat by a single-reference theory. The barrier heights obtained from these multireference computations agree closely with one another, being approximately 30 kJ/mol.

We present here streamline plots and numerically integrated ring current susceptibilities for the square structure of cyclobutadiene together with those for the rectangular structure. Some earlier works have discussed the aromaticity of rectangular C_4H_4 using different aromaticity measures and found it to be antiaromatic.^{56,69} Karadakov did aromaticity computations at the CASSCF level using the NICS criterion for the ground and excited states of benzene and cyclobutadiene,⁷⁰ but considering that NICS is a derived property of the ring current theory,⁷¹ our plots and numerical values give more reliable estimates of the antiaromaticity of this important system. Figures 1 and 2 show plots of the induced current strengths on a grid, demonstrating graphically the inability of a single-reference method to properly describe this system at the square geometry. In Table 1, we report the integrated ring

approach to deal with the open-shell nature of the square system.

To strengthen our claim regarding the increase in antiaromaticity going from the rectangular to the square geometry, we computed the ring current susceptibility values along the automerization pathway (Figure 3) and found that the amount of antiaromaticity increases monotonically from the rectangular to the square geometries. The automerization pathway is adopted from the work of Li and Paldus,⁶⁷ wherein we keep the sum of the adjacent bonds at twice the equilibrium bond length of 1.4668 Å for the square geometry. Thus we vary the length of one of the shorter bonds from 1.2668 Å to 1.6668 Å, thereby giving a section of the potential energy surface, which goes from one single-reference structure to another via a genuinely multireference structure. In Figure 3 we plot the integrated ring current susceptibility through this cross section. We compare the susceptibility values obtained from CASSCF-(4,4), CASSCF(2,2), and HF level computations obtained using the aug-cc-pVDZ basis set. Figure 3 shows that the inclusion of all four π orbitals formed by the p_z orbitals from the carbon atoms into the active space gives considerable correlation effects on the integrated ring current susceptibility values, though the back-correction provided by the (12,12) CAS suggests that the (4,4) CAS is too small to give a balanced description of the correlation effects in the molecule.

4.2. Benzyne. Aromatic or antiaromatic biradicals are prototypical systems for assessing the applicability of our implementation. A biradical system, with an open-shell singlet ground state, requires the use of a multiconfigurational theory and the effect of static correlation on the electron delocalization in these systems is of particular interest. For our study we have chosen to examine three isomers of the didehydrobenzenes (benzyne)s because they are aromatic and have open-shell character. There has been a renewed interest in the *ortho*-, *meta*-, and *para*-benzyne after the emergence of ene-diyne-based⁷² DNA cleaving agents⁷³ and the possibility of these aromatic diradicals being intermediates in such reactions.⁷⁴ These reactions are proposed to occur via an hydrogen abstraction pathway, wherein the diradical abstracts H atoms from the sugar phosphate in DNA and other allied systems. A detailed study of the electronic structure of these molecules may therefore shed some light on the properties of these molecules.

Table 1. Induced Ring Current Susceptibility (in nA/T) in Cyclobutadiene

molecule	HF	B3LYP	CAS(2,2)	CAS(4,4)	CAS(12,12)
CBD (rectangular)	-20.7	-20.7	-18.2	-13.3	-15.9
CBD (square)	367.2	301.5	-64.5	-33.1	-52.7

current susceptibility values at the CASSCF levels of theory using Dunning's aug-cc-pVDZ basis set and various active spaces and compare it with the HF and KS DFT results using the B3LYP exchange-correlation functional. These results give numerical evidence for the drastic increase in antiaromaticity for the square geometry compared to the rectangular geometry, highlighting the importance of a genuine multiconfigurational

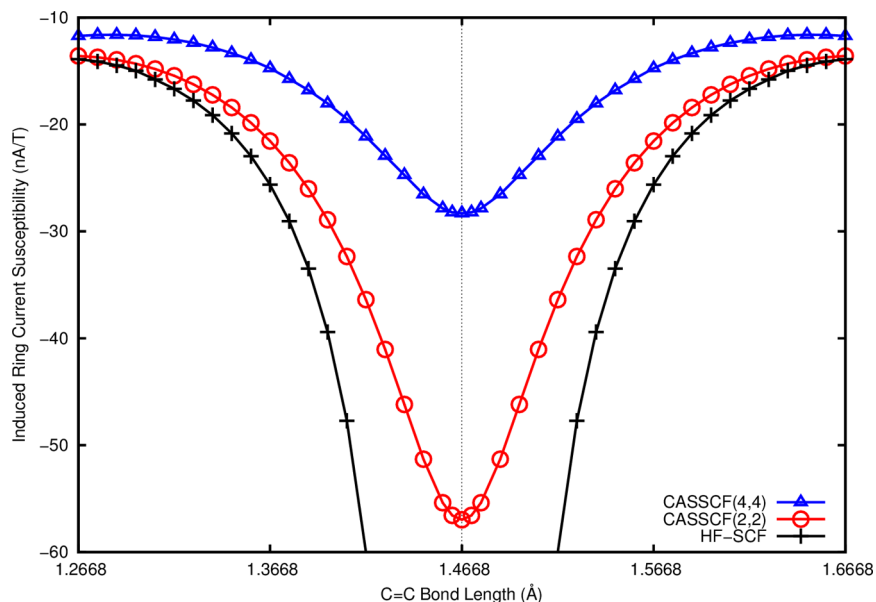


Figure 3. Integrated ring current susceptibility values through a cross section of the automerization surface for cyclobutadiene.

Table 2. Induced Ring Current Susceptibility (in nA/T) in Benzene and Benzyne

molecule	HF	B3LYP	CASSCF(2,2)	CASSCF(8,8)	NICS ^a (total)	NICS(π) ^b	$\Delta\chi^c$	ASE [kcal/mol] ^d	Λ [ppm cgs] ^e
benzene	13.2	12.4	13.5	13.5*	-8.8	-20.7	-	33.9	-16.4
<i>o</i> -benzyne	14.1	13.8	13.5	13.5	-18.4	-22.2	-52.28	34.9	-16.9
<i>m</i> -benzyne	12.8	11.2	12.7	12.2	-17.9	-23.0	-55.29	28.2	-13.8
<i>p</i> -benzyne	20.1	18.3	14.1	14.3	-28.1	-23.1	-58.81	-	-

*CASSCF(6,6) for benzene. In this work the structures have been optimized at the CASSCF(8,8)/aug-cc-pVDZ level. ^aNucleus Independent Magnetic Shifts (NICS) values are taken from ref 83. Total NICS for points located at the geometrical centers of the rings computed at the B3LYP/6-311+G** level (with structures optimized at the B3LYP/6-311+G** level of theory). ^bNICS(π) denotes dissected π contribution at the geometrical center of the ring.⁸³ ^cAverage in-plane diamagnetic susceptibility, $\Delta\chi$, at the CASSCF(8,8)/cc-pVDZ level for the same geometries as in ^a.⁸³ ^dASE stands for aromatic stabilization energy.⁸³ ^e Λ denotes magnetic susceptibility exaltation.⁸³

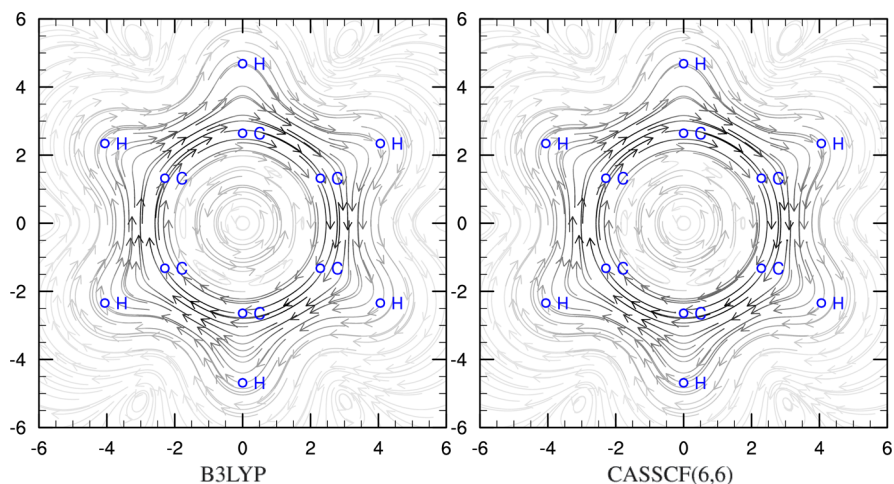


Figure 4. Comparison of MICD plots for benzene plotted 1 a_0 above the molecular plane.

A large number of theoretical studies on the benzyne systems focused on thermochemistry, obtaining good equilibrium geometries and singlet-triplet splittings.^{75,76} These studies have been carried out including dynamic correlation in a single-reference framework⁷⁷⁻⁷⁹ and also at the CASSCF⁸⁰ or CASPT2 levels of theory.⁸¹ Recent developments in multi-reference electronic structure methods and their application to geometry optimizations have made benzyne a natural test

bed.⁸² The calculated molecular structures,^{80,79} singlet-triplet splittings,^{78,79} and heats of formation⁸¹ have provided insight into the aromatic character of the benzyne, but no dedicated study on aromaticity was undertaken before that of De Proft et al.⁸³ De Proft et al. employed four different aromaticity indices in their study, namely magnetic anisotropy, magnetic susceptibility exaltations, nucleus-independent chemical shifts (NICS), and aromatic stabilization energies (ASE), all

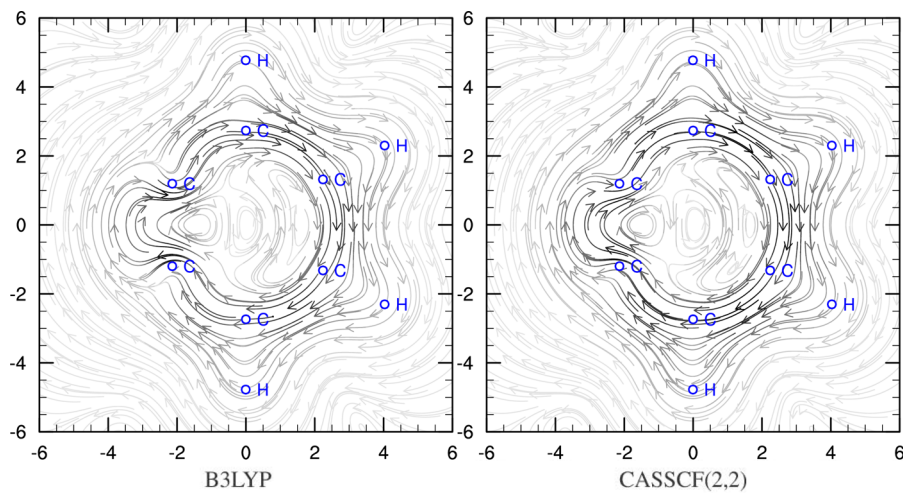


Figure 5. Comparison of MICD plots for *ortho*-benzyne plotted $1 \text{ } a_0$ above the molecular plane.

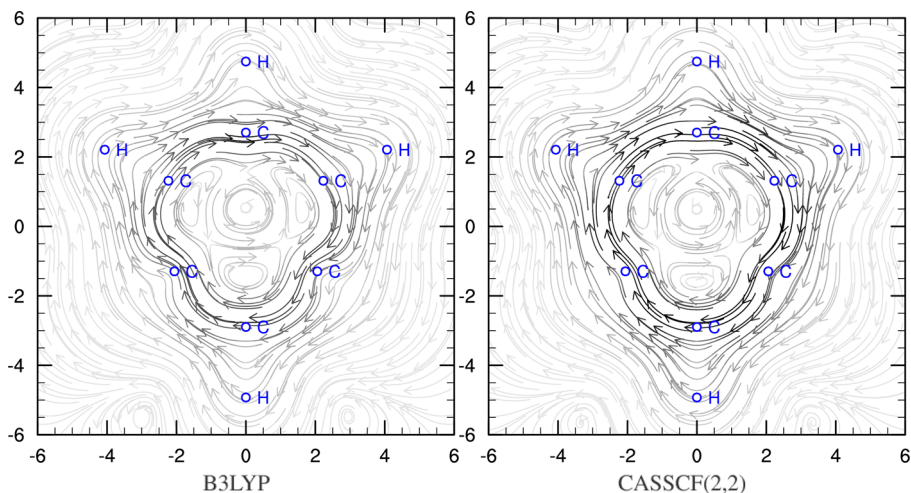


Figure 6. Comparison of MICD plots for *meta*-benzyne plotted $1 \text{ } a_0$ above the molecular plane.

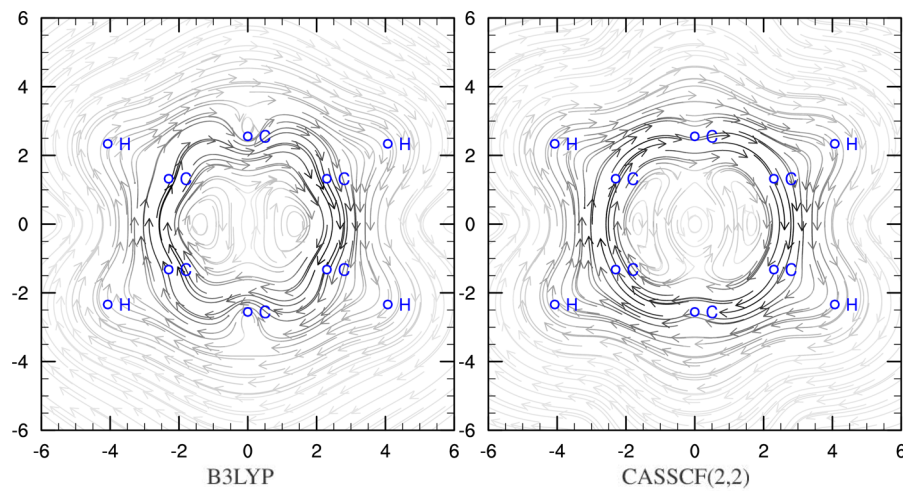


Figure 7. Comparison of MICD plots for *para*-benzyne plotted $1 \text{ } a_0$ above the molecular plane.

computed using DFT. Consensus is reached by all the above-mentioned methods that *para*-benzyne is the most aromatic among the three, but considerable discord remains between the methods in the relative ordering of the *ortho*- and the *meta*-isomers. While total NICS values, both in the molecular plane

and 1 \AA above, suggest that the *ortho*-isomer is more aromatic than the *meta*-isomer, these results also being supported by magnetic susceptibility exaltations and ASE, the anisotropy values (also computed at the CASSCF/cc-pVDZ level on geometries optimized at the BLYP/6-311+G** level) contra-

dict this result, placing the *meta*-isomer higher than the *ortho*-isomer on the aromaticity scale. The latter finding is supported by dissected NICS(π), in which only the π -orbital contribution is included in the NICS(0) values, measured at the center of the ring plane.

In this work we try to shed some light on this issue by calculating magnetically induced current densities at various levels of theory, namely, HF, DFT (B3LYP), CASSCF(2,2), and CASSCF(8,8) using the aug-cc-pVDZ basis sets on geometries optimized at the CASSCF(8,8)/aug-cc-pVDZ level of theory. All our calculations, be it at the single or multiconfigurational level, find the *meta*-isomer to be less aromatic than the *ortho*-isomer. Table 2 lists the values of the integrated ring current susceptibilities together with values from other aromaticity indices. The streamline plots as shown in Figures 4, 5, 6, and 7 clearly demonstrate the overall diatropic flow of the induced currents and also demonstrate the need for a multiconfigurational theory to provide a balanced description of the electron density for systems with unpaired electrons. It can be seen that the single-reference method would try to localize the electron density and form a bond between the free-radical centers, thus affecting the overall aromaticity by hampering delocalization. This shortcoming is alleviated even by the use of a minimal active space of 2 electrons in 2 orbitals, which allow the electrons to remain as free radicals and contributing to a better description of the degree of aromaticity induced by the biradical character.

5. CONCLUDING REMARKS

We have presented the implementation of an aromaticity index based on the first-order magnetic response for multiconfigurational self-consistent-field wave functions. This enables us to extend the magnetic criterion for aromaticity to systems which require a multiconfigurational description. As for the shortcomings of the method, the foremost is the lack of dynamic correlation. Our implementation can thus be seen as a first step toward more sophisticated and elaborate multireference perturbation and coupled-cluster methods for the determination of magnetically induced current densities.

We would like to mention a few other possible applications for our implementation. Ruud et al.^{51,84} have pointed out the discrepancy in the calculated and experimental values of magnetizabilities. It has been suggested that this can be attributed to solvent effects. Our current implementation would give us the opportunity to probe the changes in magnetizabilities as well as visualize the magnetically induced currents in real space, thus potentially giving insight into the origins of the observed paramagnetic shift observed when going from the gas to the liquid phase. We expect this implementation to provide valuable insights into the origins of the observed changes in the magnetizability of systems at different bond lengths and intermolecular separations, for systems containing multiple bonds (which cannot be described well by simple modifications of the Pascal's Rule⁵¹). The MCSCF formalism will also allow us to directly probe the concept of excited-state aromaticity using the magnetic criterion.⁸⁵

■ AUTHOR INFORMATION

Corresponding Author

*E-mail: kenneth.ruud@uit.no.

Notes

The authors declare no competing financial interest.

■ ACKNOWLEDGMENTS

This work has been supported by the Research Council of Norway through a Centre of Excellence Grant (Grant No 179568/V30). Computer time from the Norwegian Supercomputing Program (NOTUR) is also gratefully acknowledged. S.P. would like to thank the Department of Science and Technology, Govt. of India, for his fellowship. S.P. also thanks the CTCC, University of Tromsø for the Visiting Student scholarship. The authors would like to thank Dr. Swapna Chakrabarti, Prof. Debasish Mukherjee, Dr. Małgorzata Olejniczak, and Prof. Trond Saue for stimulating discussions.

■ REFERENCES

- (1) Minkin, V. I.; Glukhovtsev, M. N.; Simkin, B. Y. *Aromaticity and Antiaromaticity*; John Wiley & Sons: New York, 1994.
- (2) Krygowski, T. M.; Cyrański, M. K.; Czarnocki, Z.; Hafelinger, G.; Katritzky, A. R. *Tetrahedron* **2000**, *56*, 1783.
- (3) Schleyer, P. v. R.; Jiao, H. *Pure Appl. Chem.* **1996**, *68*, 209.
- (4) Kekulé, A. *Bull. Soc. Chim. Paris* **1865**, *3*, 98.
- (5) Julg, A.; Francüois, P. *Theor. Chim. Acta* **1967**, *7*, 249.
- (6) Pauling, L.; Sherman, J. *J. Chem. Phys.* **1933**, *1*, 606.
- (7) Dewar, M. J. S.; Gleicher, G. J. *J. Am. Chem. Soc.* **1965**, *87*, 685.
- Dewar, M. J. S.; Gleicher, G. J. *J. Am. Chem. Soc.* **1965**, *87*, 692.
- (8) Hess, B. A., Jr.; Schaad, L. J. *J. Am. Chem. Soc.* **1971**, *93*, 305.
- Hess, B. A., Jr.; Schaad, L. J. *J. Am. Chem. Soc.* **1971**, *93*, 2413.
- (9) Erlenmeyer, E. *Ann. Chem. Pharm.* **1866**, *137*, 327.
- (10) Zhou, Z.; Parr, R. G.; Garst, J. F. *Tetrahedron Lett.* **1988**, *29*, 4843.
- (11) Pascal, P. *Ann. Chim. Phys.* **1910**, *19*, 5. Pascal, P. *Ann. Chim. Phys.* **1912**, *25*, 289. Pascal, P. *Ann. Chim. Phys.* **1913**, *28*, 218.
- (12) Pauling, L.; Sherman, J. *J. Chem. Phys.* **1933**, *1*, 606.
- (13) Sondheimer, F.; Calder, I. C.; Elix, J. A.; Gaoni, Y.; Garratt, P. J.; Grohmann, K.; di Maio, G.; Mayer, J.; Sargent, M. V.; Wolovsky, R. *Chem. Soc. Spec. Publ.* **1967**, *21*, 75.
- (14) Dauben, H. J., Jr.; Wilson, J. D.; Laity, J. L. *J. Am. Chem. Soc.* **1968**, *90*, 881. Dauben, H. J., Jr.; Wilson, J. D.; Laity, J. L. *J. Am. Chem. Soc.* **1969**, *91*, 1991.
- (15) Schleyer, P. v. R.; Jiao, H.; Glukhovtsev, M. N.; Chandrasekhar, J.; Kraka, E. *J. Am. Chem. Soc.* **1994**, *116*, 10129.
- (16) Schleyer, P. v. R.; Maerker, C.; Dransfeld, A.; Jiao, H.; van Eikema Hommes, N. J. R. *J. Am. Chem. Soc.* **1996**, *118*, 6317.
- (17) Luzzetti, P.; Zanazi, R. *Chem. Phys. Lett.* **1981**, *80*, 533.
- (18) Jusélius, J.; Sundholm, D. *Phys. Chem. Chem. Phys.* **1999**, *1*, 3429.
- (19) Gomes, J. A. N. F.; Mallion, R. B. *Chem. Rev.* **2001**, *101*, 1349.
- (20) Chen, Z.; Wannere, C. S.; Corminboeuf, C.; Puchta, R.; Schleyer, P. v. R. *Chem. Rev.* **2005**, *105*, 3842.
- (21) Dauben, H. J., Jr.; Wilson, J. D.; Laity, J. L. *Diamagnetic Susceptibility Exaltation as Criterion of Aromaticity*. In *Nonbenzenoid Aromatics*; Snyder, J. P., Ed.; Academic Press: New York, 1971; Vol. 2.
- (22) Bernstein, H. J.; Schneider, W. G.; Pople, J. A. *Proc. R. Soc. London, Ser. A* **1956**, *236*, 515.
- (23) Pople, J. A. *J. Chem. Phys.* **1956**, *24*, 1111.
- (24) Pople, J. A. *Mol. Phys.* **1958**, *1*, 175.
- (25) Sondheimer, F. *Acc. Chem. Res.* **1972**, *5*, 81.
- (26) Bilde, M.; Hansen, Aa. E. *Mol. Phys.* **1997**, *92*, 237.
- (27) Jusélius, J.; Sundholm, D. *Phys. Chem. Chem. Phys.* **2000**, *2*, 2145.
- (28) Luzzetti, P.; Zanazi, R. *J. Chem. Phys.* **1981**, *75*, 5019.
- (29) Jusélius, J.; Sundholm, D.; Gauss, J. *J. Chem. Phys.* **2004**, *121*, 3952.
- (30) Fliegl, H.; Taubert, S.; Lehtonen, O.; Sundholm, D. *Phys. Chem. Chem. Phys.* **2011**, *13*, 20500.
- (31) Bast, R.; Jusélius, J.; Saue, T. *Chem. Phys.* **2009**, *356*, 187.
- (32) Sulzer, D.; Olejniczak, M.; Bast, R.; Saue, T. *Phys. Chem. Chem. Phys.* **2011**, *13*, 20682.

- (33) Roos, B. O. The Complete Active Space Self-Consistent Field Method and its Applications in Electronic Structure Calculations. In *Advances in Chemical Physics: Ab Initio Methods in Quantum Chemistry Part 2, Volume 69*; Lawley, K. P., Ed.; John Wiley & Sons, Inc.: Hoboken, NJ, USA.
- (34) Yeager, D. L.; Jørgensen, P. *Chem. Phys. Lett.* **1979**, *65*, 77.
- (35) Olsen, J.; Jørgensen, P. *J. Chem. Phys.* **1985**, *82*, 3235.
- (36) Jørgensen, P.; Jensen, H. J. Aa.; Olsen, J. *J. Chem. Phys.* **1988**, *89*, 3654.
- (37) Bak, K. L.; Jørgensen, P.; Helgaker, T.; Ruud, K.; Jensen, H. J. Aa. *J. Chem. Phys.* **1993**, *98*, 8873.
- (38) Ruud, K.; Helgaker, T.; Kobayashi, R.; Jørgensen, P.; Bak, K. L.; Jensen, H. J. Aa. *J. Chem. Phys.* **1994**, *100*, 8178.
- (39) Ruud, K.; Helgaker, T.; Bak, K. L.; Jørgensen, P.; Olsen, J. *Chem. Phys.* **1995**, *195*, 157.
- (40) London, F. *J. Phys. Radium* **1937**, *8*, 397.
- (41) Wolinski, K.; Hinton, J. F.; Pulay, P. *J. Am. Chem. Soc.* **1990**, *112*, 8251.
- (42) Gauss, J.; Stanton, J. F. *J. Chem. Phys.* **1995**, *102*, 251.
- (43) Helgaker, T.; Coriani, S.; Jørgensen, P.; Kristensen, K.; Olsen, J.; Ruud, K. *Chem. Rev.* **2012**, *112*, 543.
- (44) Olsen, J.; Bak, K. L.; Ruud, K.; Helgaker, T.; Jørgensen, P. *Theor. Chim. Acta* **1995**, *90*, 421.
- (45) Dalgaard, E. *J. Chem. Phys.* **1980**, *72*, 816.
- (46) Helgaker, T.; Jørgensen, P.; Olsen, J. *Molecular Electronic Structure Theory*; Wiley & Sons: Chichester, 2000.
- (47) DALTON, a molecular electronic structure program. See: <http://www.daltonprogram.org> (accessed March 23, 2013).
- (48) Stephens, P. J.; Devlin, F. J.; Chabalowski, C. F.; Frisch, M. J. *J. Phys. Chem.* **1994**, *98*, 11623.
- (49) Dunning, T. H., Jr. *J. Chem. Phys.* **1989**, *90*, 1007.
- (50) Kendall, R. A.; Dunning, T. H., Jr.; Harrison, R. J. *J. Chem. Phys.* **1992**, *96*, 6796.
- (51) Ruud, K.; Skaane, H.; Helgaker, T.; Bak, K. L.; Jørgensen, P. *J. Am. Chem. Soc.* **1994**, *116*, 10135.
- (52) Ruud, K.; Helgaker, T. *Chem. Phys. Lett.* **1997**, *264*, 17.
- (53) Bally, T. *Angew. Chem., Int. Ed. Engl.* **2006**, *45*, 6616.
- (54) Maier, G. *Angew. Chem., Int. Ed. Engl.* **1974**, *13*, 425.
- (55) Schleyer, P. v. R.; Manoharan, M.; Wang, Z.-X.; Kiran, B.; Haijun Jiao, H.; Puchta, R.; Hommes, N. J. R. v. E. *Org. Lett.* **2001**, *3*, 2465.
- (56) Flieg, H.; Sundholm, D.; Taubert, S.; Jusélius, J.; Klopper, W. J. *Phys. Chem. A* **2009**, *113*, 8668.
- (57) Breslow, R.; Murayama, D. R.; Murahashi, S.-I.; Grubbs, R. J. *Am. Chem. Soc.* **1973**, *95*, 6688.
- (58) Wu, J. I-C; Mo, Y.; Evangelista, F. A.; Schleyer, P. v. R. *Chem. Commun.* **2012**, *48*, 8437.
- (59) Whitman, D. W.; Carpenter, B. K. *J. Am. Chem. Soc.* **1982**, *104*, 6473.
- (60) Orendt, A. M.; Arnold, B. R.; Radziszewski, J. G.; Facelli, J. C.; Malsch, K. D.; Strub, H.; Grant, D. M.; Michel, J. *J. Am. Chem. Soc.* **1988**, *110*, 2648.
- (61) Carpenter, B. K. *J. Am. Chem. Soc.* **1983**, *105*, 1700.
- (62) Huang, M.-J.; Wolfsberg, M. *J. Am. Chem. Soc.* **1984**, *106*, 4039.
- (63) Čársky, P.; Bartlett, R. J.; Fitzgerald, G.; Noga, J.; Špirko, V. J. *Chem. Phys.* **1988**, *89*, 3008.
- (64) Lefebvre, R.; Moiseyev, N. *J. Am. Chem. Soc.* **1990**, *112*, 5052.
- (65) PyNGL, developed at the National Center for Atmospheric Research. See: <http://www.pyngl.ucar.edu> (accessed March 23, 2013).
- (66) Eckert-Maksic', M.; Vazdar, M.; Barbatti, M.; Lischka, H.; Maksic', Z. B. *J. Chem. Phys.* **2006**, *125*, 064310.
- (67) Li, X.; Paldus, J. *J. Chem. Phys.* **2009**, *131*, 114103.
- (68) Das, S.; Pathak, S.; Datta, D.; Mukherjee, D. *J. Chem. Phys.* **2012**, *136*, 164104.
- (69) Schleyer, P. v. R.; Maerker, C.; Dransfeld, A.; Jiao, H.; Hommes, N. J. R. *E. J. Am. Chem. Soc.* **1996**, *118*, 6317.
- (70) Karadakov, P. B. *J. Phys. Chem. A* **2008**, *112*, 7303.
- (71) Lazzaretti, P. *Phys. Chem. Chem. Phys.* **2004**, *6*, 217.
- (72) For a review of the enediyne compounds, see: Nicolaou, K. C.; Dai, W.-M. *Angew. Chem., Int. Ed. Engl.* **1991**, *30*, 1387.
- (73) Borders, D. B.; Doyle, T. W. *Enediyne Antibiotics as Antitumor Agents*; Marcel Dekker: New York, 1995.
- (74) Wenk, H. H.; Winkler, M.; Sander, W. *Angew. Chem., Int. Ed. Engl.* **2003**, *42*, 502.
- (75) Radom, L.; Nobes, R. H.; Underwood, D. J.; Li, W.-K. *Pure Appl. Chem.* **1986**, *58*, 75.
- (76) Scheiner, A. C.; Schaefer, H. F., III; Liu, B. *J. Am. Chem. Soc.* **1989**, *111*, 3118.
- (77) Kraka, E.; Cremer, D. *Chem. Phys. Lett.* **1993**, *216*, 333.
- (78) de Visser, S. P.; Filatov, M.; Shaik, S. *Phys. Chem. Chem. Phys.* **2000**, *2*, 5046.
- (79) Debbert, S. L.; Cramer, C. J. *Int. J. Mass Spectrom.* **2000**, *1*, 201.
- (80) Wierschke, S. G.; Nash, J. J.; Squires, R. R. *J. Am. Chem. Soc.* **1993**, *115*, 11958.
- (81) Cramer, C. J.; Nash, J. J.; Squires, R. R. *Chem. Phys. Lett.* **1997**, *277*, 311.
- (82) Jagau, T.-C.; Prochnow, E.; Evangelista, F. A.; Gauss, J. *J. Chem. Phys.* **2010**, *134*, 144110.
- (83) Proft, F. D.; Schleyer, P. v. R.; van Lenthe, J. H.; Frank Stahl, F.; Geerlings, P. *Chem.—Eur. J.* **2002**, *8*, 3402.
- (84) Ruud, K.; Taylor, P. R.; Jaszunski, M. *J. Phys. Chem. A* **2000**, *104*, 168.
- (85) Baird, N. C. *J. Am. Chem. Soc.* **1972**, *94*, 4941.